A&A 468, 263–272 (2007)
DOI: 10.1051/0004-6361:20066454

Astronomy & Astrophysics

Fundamental parameters of He-weak and He-strong stars⋆,⋆⋆

L. S. Cidale[1], M. L. Arias[1], A. F. Torres[1], J. Zorec[2], Y. Frémat[3], and A. Cruzado[1]

[1] Facultad de Ciencias Astronómicas y Geofísicas, Universidad Nacional de La Plata and Instituto de Astrofísica de La Plata (CONICET), Paseo del Bosque S/N, 1900 La Plata, Buenos Aires, Argentina
e-mail: lydia@fcaglp.fcaglp.unlp.edu.ar
[2] Institut d'Astrophysique de Paris, UMR7095 CNRS, Université Pierre & Marie Curie, 98bis bd. Arago, 75014 Paris, France
[3] Royal Observatory of Belgium, 3 Av. Circulaire, 1180 Bruxelles, Belgium

Received 27 September 2006 / Accepted 15 March 2007

ABSTRACT

Context. He-weak and He-strong stars are chemically peculiar AB objects whose He lines are anomalously weak or strong for their MK spectral type. The determination of fundamental parameters for these stars is often more complex than for normal stars due to their abundance anomalies.

Aims. We discuss the determination of fundamental parameters: effective temperature, surface gravity, and visual and bolometric absolute magnitudes of He-weak and He-strong stars. We compare our values with those derived independently from methods based on photometry and model fitting.

Methods. We carried out low resolution spectroscopic observations in the wavelength range 3400–4700 Å of 20 He-weak and 8 He-strong stars to determine their fundamental parameters by means of the Divan-Chalonge-Barbier (BCD) spectrophotometric system. This system is based on the measurement of the continuum energy distribution around the Balmer discontinuity (BD). For a few He-weak stars we also estimate the effective temperatures and the angular diameters by integrating absolute fluxes observed over a wide spectral range. Non-LTE model calculations are carried out to study the influence of the He/H abundance ratio on the emergent radiation of He-strong stars and on their $T_{\rm eff}$ determination.

Results. We find that the effective temperatures, surface gravities and bolometric absolute magnitudes of He-weak stars estimated with the BCD system and the integrated flux method are in good agreement between each other, and they also agree with previous determinations based on several different methods. The mean discrepancy between the visual absolute magnitudes derived using the HIPPARCOS parallaxes and the BCD values is on average ±0.3 mag for He-weak stars, while it is ±0.5 mag for He-strong stars. For He-strong stars, we note that the BCD calibration, based on stars in the solar environment, leads to overestimated values of $T_{\rm eff}$. By means of model atmosphere calculations with enhanced He/H abundance ratios we show that larger He/H ratios produce smaller BD which naturally explains the $T_{\rm eff}$ overestimation. We take advantage of these calculations to introduce a method to estimate the He/H abundance ratio in He-strong stars. The BD of HD 37479 suggests that the $T_{\rm eff}$ of this star remains fairly constant as the star spectrum undergoes changes in the intensity of H and He absorption lines. Data for the He-strong star HD 66765 are reported for the first time.

Key words. stars: early-type – stars: chemically peculiar – stars: magnetic fields – stars: fundamental parameters

1. Introduction

Ap/Bp stars are upper main sequence objects that show an abnormal abundance enhancement of some chemical species in their atmospheres as compared to "normal" A and B dwarfs of the same effective temperature (Jaschek & Jaschek 1987a). Besides these chemically peculiar (CP) stars, which encompass classical A magnetic stars (CP1), Si, Cr and SrCrEu Ap stars (CP2) and HgMn stars (CP3), there are also CP B-type objects having abnormally weak or abnormally strong lines of He I. They are called He-weak (CP4) and He-strong stars, respectively. The He-strong stars are considered the high-temperature extension of classical Ap/Bp stars (Osmer & Peterson 1974).

Most CP stars have strong and variable dipolar or quadrupolar magnetic fields, whose interaction with the gravitational and radiative diffusion processes is assumed to induce non-homogeneous distributions of different chemical elements. However, in some cases, this mechanism alone cannot account for all abundance and isotopic anomalies (Proffitt et al. 1999).

Accurate values of fundamental parameters (effective temperature, surface gravity, visual and bolometric absolute magnitudes) are of crucial importance to study the evolutionary status of stars and the physical processes that take place in their atmospheres/interiors. They also enable us to explore the appearance of their anomalies in connection with the physical characteristics of their local galactic environment (kinematics, magnetic fields, average content of chemical elements, etc.). In particular, these parameters are useful to study the evolution of magnetic fields in CP stars.

Since the photospheric abundance anomalies modify the flux distribution, the colours of CP stars can be affected by the concomitant blanketing effect. The use of standard methods based on calibrations of colour indices in terms of $T_{\rm eff}$ can then lead to erroneous results. Several authors have already discussed the difficulties of determining the effective temperature of these stars (e.g. Leckrone et al. 1974; Hauck & North 1993; Napiwotzki et al. 1993; Sokolov 1998). From these studies it is apparent that

⋆ Observations taken at CASLEO, operating under agreement of CONICET and the Universities of La Plata, Córdoba and San Juan, Argentina.

⋆⋆ Tables 1–11 and Appendix A are only available in electronic form at http://www.aanda.org

the use of the Geneva or Strömgren photometry to determine $T_{\rm eff}$ of CP stars is much more complex than for normal stars. Napiwotski et al. (1993) have discussed different uvbyβ photometric calibrations to derive $T_{\rm eff}$ and $\log g$. They recommended the use of Moon & Dworetsky's (1985) calibration corrected for gravity deviations.

Other alternative methods have also been proposed. For instance, the infrared flux method (IRFM) which minimizes the blanketing effect (Blackwell & Shallis 1977), measures the ratio of the total integrated flux to a monochromatic IR flux. This method is often used to determine angular diameters and effective temperatures of normal as well as of peculiar stars. Very frequently, the fundamental parameters are also determined by fitting synthetic spectra to the observed absolute energy distributions, or to line profiles, particularly the Hβ line. For CP2 stars, which are generally too blue for their spectral type, a supplementary correction to the effective temperature is needed (Stepień & Dominiczak 1989).

Sokolov (1998) proposed the Balmer continuum slope near the Balmer jump as a tool to determine the $T_{\rm eff}$ of CP stars. The method takes advantage of the fact that this slope is quite similar for normal and chemically peculiar main sequence stars. Although this method is easy to apply, it requires the stellar spectrophotometry to be corrected both for ISM reddening and for possible effects due to the abnormal energy distribution of CP stars.

The surface gravity parameter $\log g$ is often determined through theoretical line profile fittings or by using evolutionary tracks. To enter the evolutionary tracks the absolute bolometric magnitude $M_{\rm bol}$ and $T_{\rm eff}$ of stars are needed. Most frequently, $M_{\rm bol}$ is determined with photometric data and trigonometric parallaxes which provide the visual absolute magnitude that, in turn, is transformed into $M_{\rm bol}$ with the help of a bolometric correction calibration (North et al. 1997; Gómez et al. 1998; Hubrig et al. 2000; Kochukhov & Bagnulo 2006).

Not only are these methods difficult to apply to CP stars but also none of them give simultaneously $T_{\rm eff}$, $\log g$, $M_{\rm V}$ and $M_{\rm bol}$. Particularly, a) the photometry-based methods need to take into account line blanketing effects, or they rely on corrections from chemical anomalies that are applied to colours; b) the measurement of the Balmer continuum slope is based on data previously corrected for energy redistributions and/or reddening effects; and c) the determination of visual absolute magnitudes from where the bolometric magnitudes are obtained, needs well-determined parallaxes and effective temperatures.

Since most of these methods were applied to CP2 and CP3 categories, in the present contribution we focus our attention on He-weak and He-strong type stars. We note that information on He-strong stars is particularly scarce. In this work, we propose the use of the BCD spectrophotometric system (Barbier & Chalonge 1941; Chalonge & Divan 1952) as an alternative tool to infer spectral types, effective temperatures, surface gravities, visual and bolometric absolute magnitudes of CP stars. This method has the advantage of being based on direct measurable quantities of the continuum energy distribution in wavelengths near the the Balmer discontinuity (BD), which do not need corrections for interstellar and/or circumstellar extinctions and cannot be altered for beforehand unknown chemical anomalies. These quantities are strongly sensitive to the ionization balance of stellar atmospheres, so that they are excellent indicators of $T_{\rm eff}$ and $\log g$. Since these parameters certainly depend somehow on the chemical properties of stars, it seems useful to inquire whether or not we can also draw from them quantitative indications on their chemical anomalies.

In Sect. 2 we present the observational material. In Sect. 3 we give a summary about the BCD spectrophotometric system and complementary techniques used to test against the BCD system. Section 4 is devoted to the determination of fundamental parameters of 20 He-weak stars with the BCD system. We also include our determinations of effective temperatures, angular diameters and bolometric magnitudes done with the integrated flux method. We discuss the results with those obtained elsewhere independently. Section 5 gives fundamental parameters derived for 8 He-strong stars. Non-LTE model low resolution stellar spectra are also used to obtain the effective temperature and to analyze the effect of enhanced He/H abundance ratio on the BD. We discuss the difficulties encountered in determining the fundamental parameters of He-strong stars and the variation of HD 37479 spectrum mainly in view of its $T_{\rm eff}$ estimate. Section 6 shows the evolutionary status of the studied He-peculiar stars. Due to the variability observed in the He-strong group we add an appendix containing line equivalent widths. Conclusions are given in Sect. 7.

2. Observations

We obtained low resolution spectra of 28 CP stars: 20 He-weak and 8 He-strong stars (see Table 1). Most stars were observed only once. Observations were carried out at the Complejo Astronómico El Leoncito (CASLEO), San Juan, Argentina, with the 2,15 m telescope and the Boller & Chivens spectrograph on August 30–31, September 1–3 and September 28–30, 2004, and on January 18–19, 2006. We used a 600 l mm^{-1} grating (# 80), a slit width of 250 μ and a CCD detector of 512 × 512 pixels. The obtained spectra cover the range 3400–4700 Å with an effective resolution of 4.53 Å each 2 pixels.

Bias, flat field, He-Ne-Ar comparison and spectrophotometric flux standard star spectra were also secured to perform wavelength and flux calibrations. The reduction of observations was made with the IRAF[1] software package (version 2.11.3) and all the spectra were corrected from atmospheric extinction.

3. The methods

3.1. The BCD spectrophotometric system

The fundamental parameters of the program stars were mainly derived by using the BCD spectrophotometric system. This system is based on the observable parameters (λ_1, D). D measures the Balmer jump at λ3700 Å and it is a strong indicator of the effective temperature. λ_1 gives the mean spectral position of the Balmer jump and it is related to the surface gravity.

The BCD spectrophotometric system has several advantages: 1) it is not affected either by interstellar or circumstellar extinction (Zorec & Briot 1991); 2) it is based on measurable parameters of the visual continuum energy distribution near the BD which are thus related, on average, to physical properties of deeper photospheric layers than any classification system based on spectral line measurements; 3) it is possible to derive information on most of the fundamental parameters; 4) this method is easy and direct to apply; and 5) it can be applied with high accuracy to normal and many peculiar classes of B-type stars. Zorec & Briot (1991), Cidale et al. (2001) and Zorec et al. (2005)

[1] IRAF is distributed by the National Optical Astronomy Observatory, which is operated by the Association of Universities for Research in Astronomy (AURA), Inc., under cooperative agreement with the National Science Foundation.

applied it successfully to Be and B[e] objects, even though these objects may display a second BD that can be either in emission or in absorption (Divan 1979).

To determine the parameter $D = \log(F_{+3700}/F_{-3700})$ we normalize the observed energy distribution with a Planckian function, which rectify the energy distribution at both sides of the BD, and then, we extrapolate the Paschen continuum to obtain the flux at F_{+3700}. To determine F_{-3700}, we use the flux level where the higher members of Balmer lines merge together. The use of Balmer lines to determine the low level of the Balmer jump has the advantage of giving an estimate of the BD which is not affected by possible variations of the intensity of the Balmer continuum.

We have measured D and λ_1 for the program stars and determined their spectral type, $T_{\rm eff}$, $\log g$, and absolute magnitudes $M_{\rm V}$ and $M_{\rm bol}$ (see details in Sects. 4 and 5) using the respective calibrations of (λ_1, D) by Divan & Zorec (1982), Zorec (1986), and Zorec & Briot (1991). The uncertainties on $T_{\rm eff}$, $\log g$, $M_{\rm V}$ and $M_{\rm bol}$ are mainly related to the errors of the BCD observational quantities (λ_1, D). Typical values are $\sigma(D) \lesssim 0.015$ dex and $\sigma(\lambda_1) \sim 5$ Å, which produce $\Delta T_{\rm eff} \sim \pm 500$ K for the late B-type stars and ± 1500 K for the early B-types ($T_{\rm eff} > 20\,000$ K), $\Delta \log g \sim \pm 0.2$ dex, and $\Delta M \sim \pm 0.3$ mag both for $M_{\rm V}$ and $M_{\rm bol}$.

3.2. The integrated-flux method

In addition to the BCD classification system we used the integrated-flux method to derive fundamental parameters for those He-weak stars of our program with absolute fluxes observed over a wide spectral range. We perform a determination of the effective temperature, angular diameter (θ), and bolometric magnitude by means of the relation:

$$F_{\rm bol} = (\theta^2/4)\sigma_{\rm \check{S}B} T_{\rm eff}^4 \qquad (1)$$

where $F_{\rm bol}$ is the absolute bolometric flux reduced to the distance to the Earth and corrected for interstellar extinction; $\sigma_{\rm \check{S}B}$ is the Štefan-Boltzmann constant. Relation (1) is iterated starting with an approximate $T_{\rm eff}$ until the difference between two succesive iterations becomes $\Delta T_{\rm eff} \lesssim 1$ K. This implies from 10 to 30 iteration steps. At each step, θ is calculated using the $F_\lambda/F_{\rm model}$ ratio of fluxes in the wavelength interval $\lambda\lambda 7000$–8000 Å. The $F_\lambda/F_{\rm model}$ ratios are fairly insensitive to $\log g$. The observed fluxes F_λ are corrected for ISM extinction and the $F_{\rm model}$ corresponds to the running $T_{\rm eff}$. At each step we also determine the amount of non-observed far-UV and far-IR energy as a function of the $T_{\rm eff}$ under iteration using LTE models (Kurucz 1992), which we add to the integrated observed flux to obtain $F_{\rm bol}$. The wavelength interval of observed absolute fluxes ranges from 1300 Å to 1 μm. The fluxes are observed in the far-UV by the TD1 and IUE satellites, and from visible to near-IR with the 13-colour narrow band photometry calibrated in absolute fluxes (Johnson & Mitchell 1975).

3.3. Model fitting

In the case of He-strong stars we also determine $T_{\rm eff}$, and $\log g$ by computing NLTE synthetic spectra with the TLUSTY and SYNSPEC computer codes (Hubeny & Lanz 1995, and the references therein) assuming H-He model atmospheres and He/H ratios of 0.1, 0.2, 0.5 and 1.0. The atomic models we used are basically those provided on the TLUSTY website for H I (9 levels), He I (20 individual levels) and He II (20 levels). The Stark broadening of the He I transitions close to the (1s2p) 3Po ionization limit is taken from Dimitrijevic & Sahal-Brechot (1984, 1990), or it is computed using an approximate relation proposed by Freudenstein & Cooper (1978). In all cases, a microturbulent velocity of 2 km s^{-1} is assumed. To have synthetic spectra comparable with the ones observed at CASLEO, we resampled them to the resolution of the observed energy distributions.

4. He-weak stars

Table 2 gives measurements and fundamental parameters derived from the BCD spectrophotometric system. Table 3 reproduces the values of the fundamental parameters derived by using integrated absolute fluxes.

HD 125823 is the only star whose He I lines vary in strength between anomalously weak and anomalously strong. It was included in Table 2 because the star presented a He-weak phase at the date of our observations.

4.1. $T_{\rm eff}$ determination

In order to test the accuracy of the BCD effective temperatures a comparison with the values obtained by other methods is performed. Table 4 shows the effective temperatures with their corresponding uncertainties (when available) derived from the BCD system and from the literature.

Except for few stars, the effective temperatures derived with the BCD method have no significant differences with the values derived from Geneva and other multicolour photometric systems, the IRFM and LTE line-blanketed models. The mean discrepancies found between our data and those derived by other authors are lower than 800 K. The best agreement is obtained with the IRFM (Lanz 1985), the mean temperature difference being $|\Delta\ T_{\rm eff}| \sim 500$ K. We have also obtained a good agreement between our own determinations of $T_{\rm eff}$(IF) by means of the integrated-flux method and the BCD system. Comparing Tables 2 and 3, we found a mean value of $\Delta T_{\rm eff} = \pm 700$ K.

Figure 1 displays the comparison of our $T_{\rm eff}$(BCD) values vs. $T_{\rm eff}$(G) (crosses), $T_{\rm eff}$(KB) (open circles), and $T_{\rm eff}$(IF) (open triangles). In the same figure, it is also plotted a reference line with slope 1. We selected the mentioned works to perform the comparison, since the number of stars in common is large. The good correlation found between the BCD system and other methods confirms that the BD of He-weak stars behaves like that observed in normal B stars. For these stars we can then safely use the existent calibrations, done for He/H ≈ 0.1, to determine their fundamental parameters.

From our results we conclude that the behaviour of the Balmer jump in He-weak stars is different from that of Ap stars (CP2 group). The photometric anomalies of Ap stars (Gerbaldi et al. 1974; Hauck & North 1982) may introduce noticeable differences between the BCD and MK spectral classifications (Chalonge & Divan 1977).

4.2. The surface gravity

Surface gravity determinations for He-peculiar stars are hardly common. Hunger & Groote (1999) determined $\log g$ values from HIPPARCOS parallaxes together with tracks from stellar evolution, Leone & Manfrè (1996) estimated values using synthetic H line profiles while Leone et al. (1997) used Moon & Dworetsky's (1985) calibration and applied the corrections suggested by Napiwotzki et al. (1993). Table 5 compares,

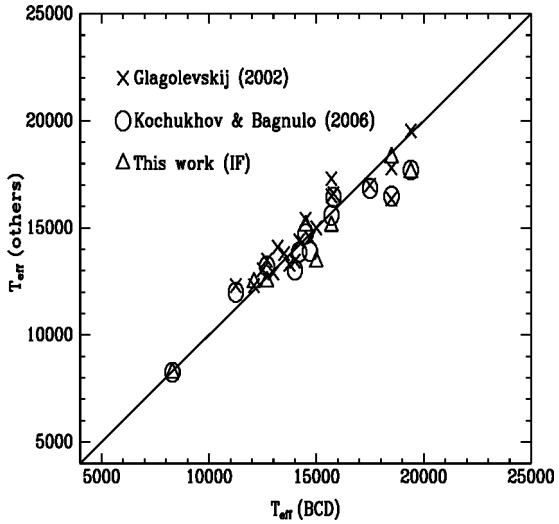

Fig. 1. Comparison of the effective temperatures derived from the BCD system with those obtained photometrically by Glagolevskij (2002), Kochukhov & Bagnulo (2006) and in this work with the integrated flux method.

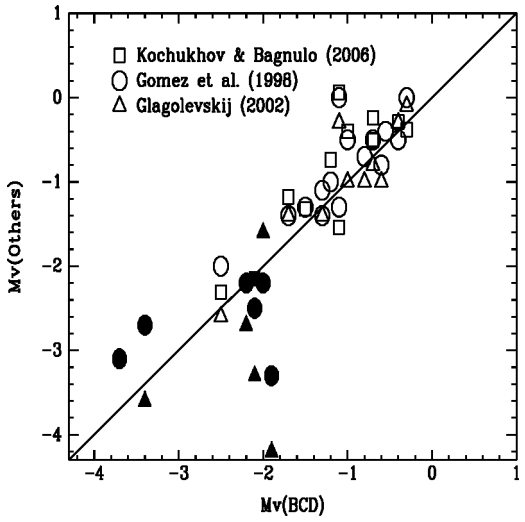

Fig. 2. Comparison of the visual absolute magnitudes derived from the BCD system with those derived by Gómez et al. (1998), Glagolevskij (2002) and Kochukhov & Bagnulo (2006). He-weak stars are represented by open symbols and He-strong stars by filled symbols.

for each object, the log g values determined by means of the BCD system with those derived by the above mentioned works. We find an excellent agreement with the values given by Hunger & Groote (1999), $|\Delta \log g| < 0.13$ dex, for 11 stars in common and a good agreement with Leone's works, $|\Delta \log g| = 0.23$ dex for six stars in common.

4.3. Visual and bolometric absolute magnitudes

Average absolute magnitudes for Ap/Bp stars were obtained by North et al. (1997) and Mégessier (1988a), and for individual objects were reported by Gómez et al. (1998) and Kochukhov & Bagnulo (2006). Using photometric measurements and HIPPARCOS astrometric data, Gómez et al. (1998) obtained that the He-weak stellar group has $M_V \approx -0.2$ mag and that the intrinsic dispersion varies from 0.6 to 0.8 mag. All these stars are clearly distributed in the Gould Belt and their kinematic behaviour is similar to that of the non-peculiar thin disk stars younger than about 10^9 years.

In our sample of 20 He-weak stars, 16 of them have absolute magnitudes determined by the LM algorithm (Gómez et al. 1998), 10 are in common with Glagolevskij (2002) and 11 are in common with Kochukhov & Bagnulo's (2006) work (see Table 6). Our determinations of visual absolute magnitudes are in a very good agreement with those obtained by the authors mentioned above (see Fig. 2). The mean discrepancy between the BCD method and the LM algorithm for the He-weak stars is 0.26 mag. We also found a good agreement with M_V obtained by Kochukhov & Bagnulo (2006), $\Delta M_V = \pm 0.3$. Instead, the mean discrepancy between the bolometric magnitudes derived from the BCD system and the values given by Glagolevskij (2002), using the parameter β of the multicolour photometry, is slightly larger ~0.44 mag. This discrepancy may be related to the bolometric correction, since when transforming the bolometric magnitudes obtained by Glagolevskij (2002) into visual absolute magnitudes (which are given in Table 6), the discrepancy become smaller.

Comparing the bolometric absolute magnitudes obtained by us with the BCD system and the integrated-flux method, we find a mean discrepancy $\Delta M_{bol} = \pm 0.5$ mag. However, a noticeable disagreement appears for HD 144661 and for the He-variable HD 125823. The large difference in the M_{bol} observed for HD 144661 cannot be recovered by simply changing the color excess $E(B-V)$; by doubling the $E(B-V)$ the bolometric luminosity would increase $\Delta L/L \sim 0.5$, while we need $\Delta L/L \sim 3.4$ to make both estimates agree. Therefore, we may suggest that some undetected flux fading is taking place. This star deserves perhaps further thorough analysis.

5. He-strong stars

The shape of the Balmer continuum of He-strong stars is somewhat different from that predicted by models with standard solar helium abundances. The He-strong spectra exhibit intense He I lines and a remarkable convergence of the last members of the series to the bound free discontinuity at 3422 Å, which corresponds to the ionization of the 2–3 Po level (see Figs. 3 and 4). The He-strong stars deserve a special discussion. They may display Hα emission and spectroscopic and photometric variability. Not only do they show variations in line intensities, radial velocities, luminosity and colours but also in the magnetic field strength (Renson et al. 1991).

We have attempted at determining fundamental parameters of these objects by means of the BCD system. However, due to the strong He I lines, a precise determination of the Paschen continuum level becomes difficult. Nevertheless, the continuum fluxes at $\lambda\lambda$4055 and 4566 Å are unaffected by strong line absorptions (Adelman & Pyper 1985). Thus, we use these points, together with the last members of the Balmer line series as references to determine the Balmer jump. Table 7 gives our (λ_1, D) measurements and the corresponding fundamental parameters. Data for the He-strong star HD 66765 is scarce and spectrophotometric measurements are published for the first time.

The energy distributions of the observed He-strong stars were fitted with the TLUSTY and SYNSPEC computing codes to have another independent effective temperature estimate. All models were convolved with a rotational broadening function for the respective stellar $V \sin i$ parameters. In Figs. 3 and 4 we show the best fit obtained for each studied star. These fits are for the

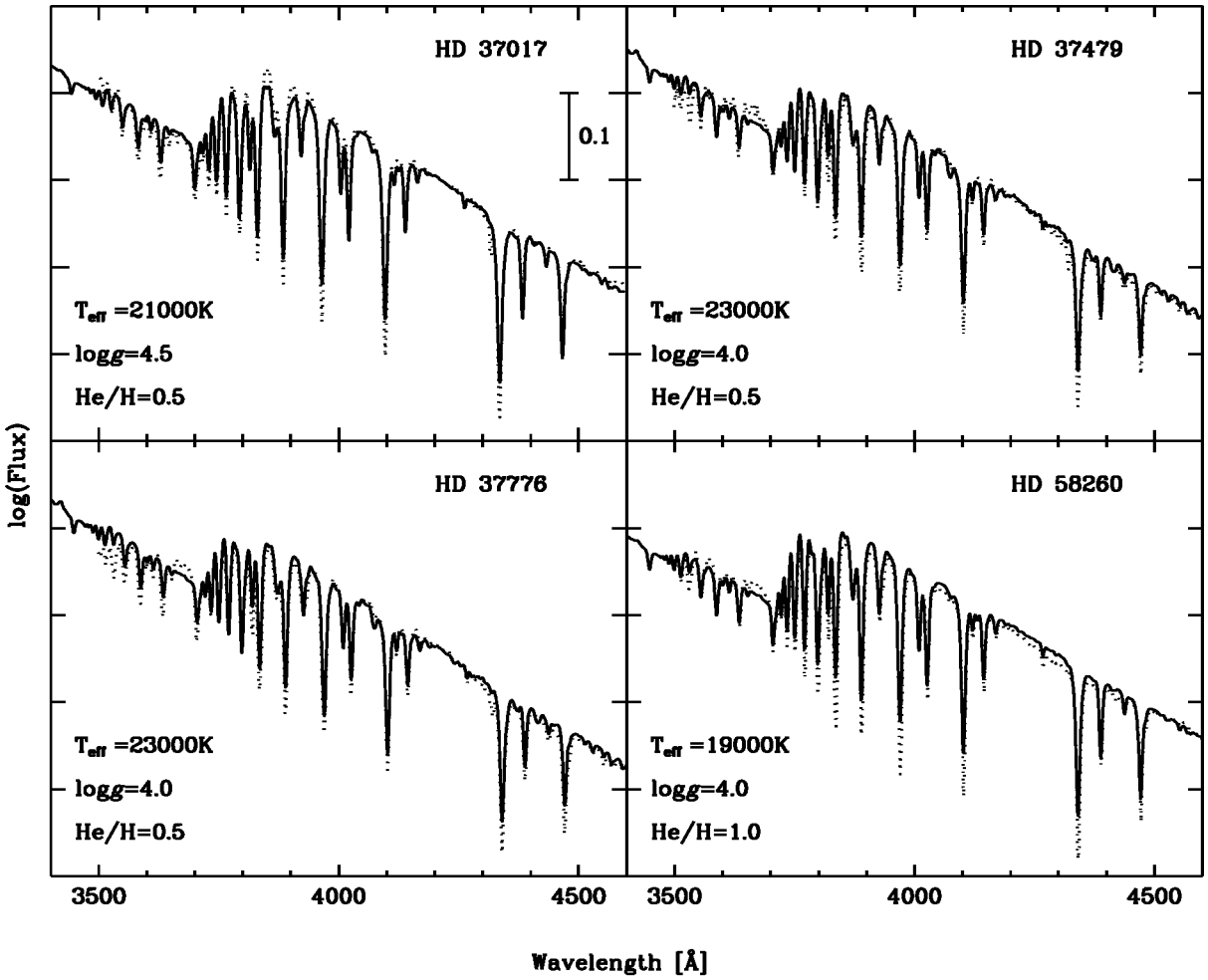

Fig. 3. Energy distributions of He-strong stars, $\log F_\lambda$, around the BD (dotted line), together with the best theoretical fitting (solid line). All spectra have the same flux scale. The convergence of the last He I line members towards 3422 Å clearly indicates the He I bound-free discontinuity.

($T_{\rm eff}$, $\log g$, H/He ratio) sets of parameters given in Table 8. The uncertainties on the parameters obtained by model fitting are on average: 1000 K for $T_{\rm eff}$ and 0.5 dex in $\log g$. However, for each He-strong star, the model that best fits the continuum energy distribution does not correctly fit the intensity of H lines. A better fitting of H lines would require models with larger atmospheric temperature gradients than the ones used in NLTE blanketed plane-parallel, in hydrostatic and radiative equilibrium, classical models. Such differences in the atmospheric temperature structure could be due not only to possible non-uniform distributions of the abnormally abundant chemical elements in latitude and/or in depth, but also to a non-negligible role of the magnetic field in cooling the upper atmospheric layers.

5.1. $T_{\rm eff}$ determination

We have sought for previous determinations of effective temperatures in the literature. Most of the $T_{\rm eff}$ values were in works that deal with only a reduced number of stars and use different techniques (Hunger & Groote 1999; Leone et al. 1997; Zboril et al. 1997; Glagolevskij 2002; Theodossiou & Danezis 1991; Adelman & Pyper 1985; Kaufmann & Theil 1980).

Table 9 compares the BCD effective temperatures with those obtained by Glagolevskij (2002), Zboril et al. (1997) and Kaufmann & Theil (1980). In this table, the non-BCD temperature determinations are from theoretical LTE model-fitting (Kurucz 1992), or from the Geneva photometry. We have chosen only these works because they treat a non negligible number of stars that are in common with our program stars. We found large discrepancies among the $T_{\rm eff}$ estimated by different authors: $2000 \lesssim \Delta T_{\rm eff} \lesssim 5000$ K. In the same way, our BCD determinations do not escape the rule. Moreover, we observed large differencies between the $T_{\rm eff}$ derived with the BCD method and the NLTE models we used. In most cases, the $T_{\rm eff}$(BCD) are systematically larger than the average $T_{\rm eff}$ from other methods. This difference deserves a more detailed discussion that will be done using the stellar atmosphere models in Sect. 5.4.

5.2. The surface gravity

As it is mentioned in Sect. 4.2, the $\log g$ values found in the literature were derived by different methods. In Table 10 we show BCD $\log g$ values together with the determinations given by other authors. The resulting mean discrepancies in $\log g$ are 0.36, 0.21, 0.37 and 0.22 dex, respectively. The values of $\log g$ quoted in the atlas of Kaufmann & Theil (1980) are taken from different sources and their uncertainties are not accessible.

The best agreement is obtained with values derived by Hunger & Groote (1999) from HIPPARCOS parallaxes together with tracks from stellar evolution.

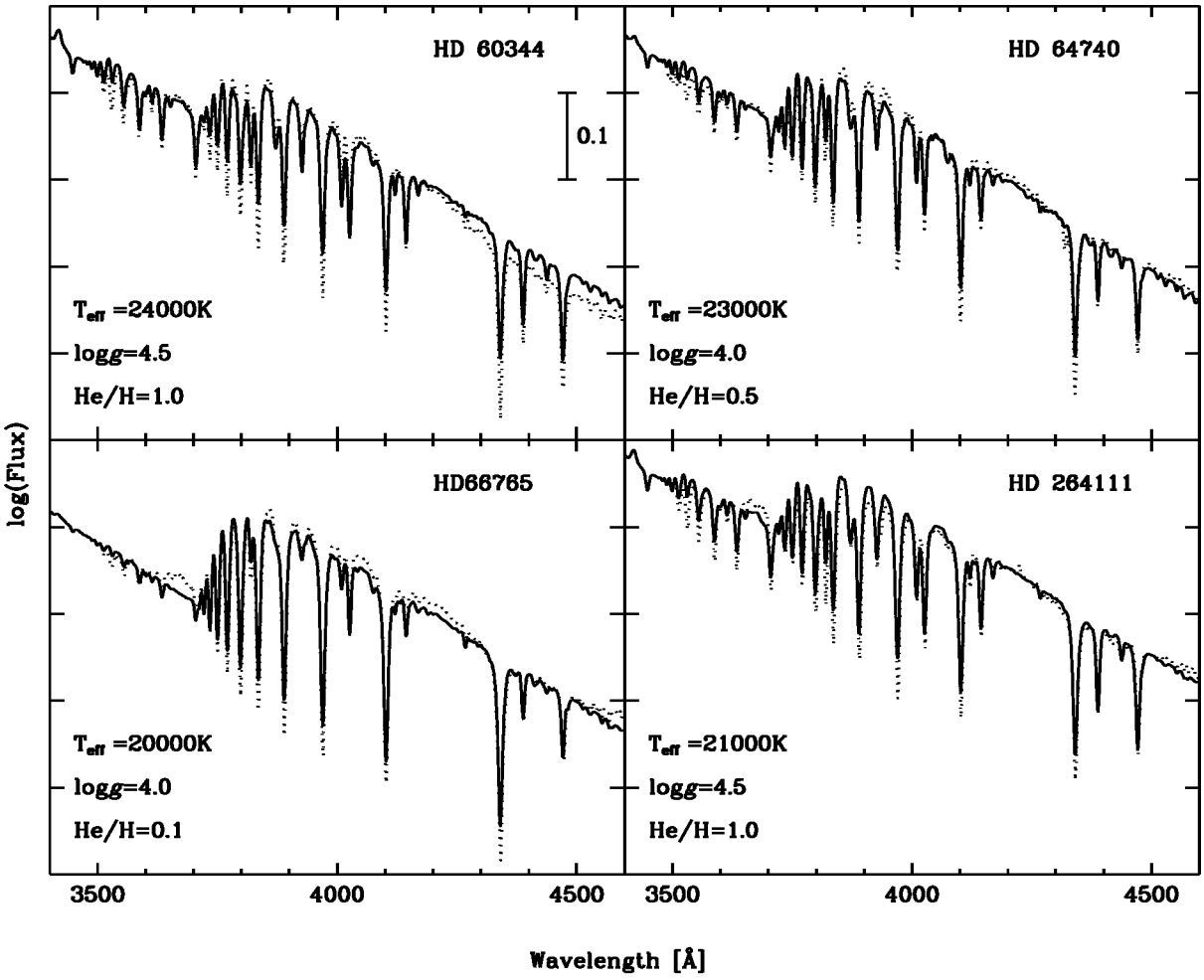

Fig. 4. Energy distributions of He-strong stars, $\log F_\lambda$, around the BD (dotted line), together with the best theoretical fitting (solid line). All spectra have the same flux scale. The convergence of the last He I line members towards 3422 Å clearly indicates the He I bound-free discontinuity.

5.3. Visual and bolometric absolute magnitudes

The He-strong group typically has $M_V \sim -1.6$ mag with a dispersion of about 1.2 mag (Gómez et al. 1998).

In our sample of 8 He-strong stars, 6 of them have absolute magnitudes determined by the LM algorithm (Gómez et al. 1998), 5 are in common with Glagolevskij (2002) and 1 with Kochukhov & Bagnulo's (2006) work (see Table 11). In Table 11, uncertainties for each value are listed when available. The values corresponding to M_V(G) were derived from M_{bol} given by Glagolevskij (2002) adding the respective bolometric correction. Our determinations of visual magnitudes are in good agreement with those obtained by the authors mentioned above (see Fig. 2, filled symbols), with the exception of HD 58260. We also found that for HD 64740 M_V(BCD) differs significantly with the value obtained by Glagolevskij (2002). We find an average discrepancy for all the stars in common of 0.53 mag between the M_V obtained with the BCD method and the LM algorithm. Comparing the values of M_{bol}(BCD) with the absolute bolometric magnitudes given by Glagolevskij (2002) we find an average discrepancy of 0.71 mag. This large difference may probably due to the bolometric correction used by Glagolevskij (2002) as we mentioned in Sect. 4.3.

5.4. Other relevant results

a) Synthetic energy distributions as a function of the He/H abundance ratio

Since BCD determinations of T_{eff} for the He-strong stars are systematically higher than those obtained by other authors, we calculate low-resolution synthetic spectra, in order to quantify the influence of the He/H abundance ratio on the emitted visual energy distribution. From these spectra we obtain the BCD parameters following the same procedure as for the empirical ones. Models are computed for effective temperatures close to those inferred empirically for He-strong stars and only for the wavelength interval of the observed low-resolution spectra.

An illustration of the effects produced on the visible energy distributions resulting from increased abundance ratios He/H is shown in Fig. 5. The spectra are slightly displaced in order to see clearly the changes in the BD, where it is apparent its shortening as He/H is higher. In this figure we can also notice the changes on the visible Balmer energy distribution induced by enhanced He free-bound transitions and the presence of strong He I line absorptions. In Table 12, the obtained D values are given as a function of the model nominal (T_{eff}, $\log g$, He/H) parameters. Thus, increased He/H ratios produce smaller values of D. This reduction has only a second order dependence with $\log g$. The

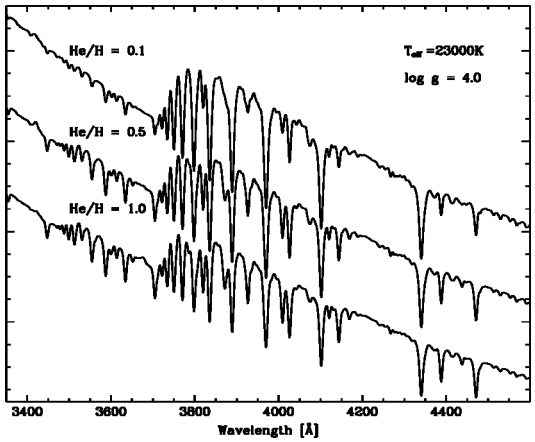

Fig. 5. Synthetic spectra displaying line and continuum changes according to increased He abundances. The spectra are slightly displaced. The NLTE model computations were performed for $T_{\rm eff}$ = 23 000 K, $\log g$ = 4.0 dex and ratios H/He = 0.1 (standard), 0.5 and 1.0.

lowering δD of the BD, averaged over $\log g$, as function of the effective temperature is given within 99.8% of approximation by the following interpolation relation:

$$\delta D = -0.056\left[1 - 0.233\left(\frac{T_{\rm eff}}{10^4}\right)^{0.974}\right]({\rm He/H}) \quad ({\rm dex}). \qquad (2)$$

Relation (2) implies that the higher the $T_{\rm eff}$ the smaller the δD. However, as $D \propto 1.0/T_{\rm eff}$, small changes in D carry big differences in $T_{\rm eff}$. Since the BCD calibrations used to estimate the effective temperatures of He-strong stars are actually made for objects with He/H $\approx$ 0.1, from Table 12 and relation (2), it becomes clear that the obtained BCD $T_{\rm eff}$ are overestimated.

Models also predict a slight brightening of stars as the He/H ratio increases. Table 13 reproduces the changes of the monochromatic magnitude at λ4250 Å with respect to models for He/H = 0.1 that stand for the "normal" or standard solar abundance ratio. We notice in Table 13 that the brightening effect is only marginally dependent on $T_{\rm eff}$ and $\log g$.

We notice that the BCD parameters, D, derived from the fitted spectra are consistent with those measured in the observed spectra. We can then assert that the actual Balmer jump of the studied He-strong stars is well-represented by the empirical D parameter. Then, entering Table 12 with the measured D values (Table 7) in columns with high He/H ratios, we recover approximately the effective temperatures obtained by fitting NLTE models (Table 8). These $T_{\rm eff}$(NLTE) values are similar to those reported by other authors (Table 9).

b) Spectral variations

We observe that HD 37479 (Fig. 6) has near-UV flux, Balmer jump and line intensity variations, while the Paschen continuum does not seem to undergo appreciable changes. The intensity of H lines increases when that of He I lines decreases and the near-UV flux is lower. A remarkable difference is found in the equivalent widths (~30%), in the line intensities, and on the He/H line ratio as measured in the spectrum obtained on 2004, Sep. 2 and in another one taken two days before (see Table A.1). In the spectrum of Sep. 2, there is a flux excess in the Balmer continuum near the BD, as compared to its level in the spectrum of two days latter. This excess is reminiscent of the second component of the BD seen in emission in some Be stars (Divan 1978). Whether this flux excess in He-strong stars is a matter of an actual emission, still remains to be proved. Nevertheless, if we estimate D with the criteria explained in Sect. 5.4a), we can see that D = 0.094 ± 0.006 dex on 2004, Sep. 2 and D = 0.107 ± 0.004 dex on 2004, Sep. 4. This implies that the stellar $T_{\rm eff}$ remains fairly unchanged when there are strong variations of He and H lines. Eventhough, the flux excess near the BD might lead to too high values of $T_{\rm eff}$ when derived by model fitting.

Table 12. Model D parameters as a function of $T_{\rm eff}$, $\log g$ and He/H abundance ratio.

$T_{\rm eff}$	$\log g$	He/H			
		0.1	0.2	0.5	1.0
		D (dex)			
17 000	3.5	0.206	0.201	0.189	0.170
	4.0	0.217	0.207	0.199	0.184
	4.5	0.218	0.215	0.207	0.191
19 000	3.5	0.176	0.169	0.156	0.140
	4.0	0.190	0.179	0.169	0.144
	4.5	0.190	0.184	0.169	0.155
21 000	3.5	0.135	0.133	0.122	0.110
	4.0	0.136	0.142	0.130	0.114
	4.5	0.158	0.151	0.140	0.123
23 000	3.5	0.111	0.110	0.104	0.098
	4.0	0.126	0.123	0.111	0.099
	4.5	0.137	0.131	0.119	0.106
25 000	3.5	0.092	0.089	0.080	0.069
	4.0	0.089	0.095	0.086	0.077
	4.5	0.107	0.103	0.090	0.077
27 000	3.5	0.080	0.077	0.071	0.063
	4.0	0.092	0.087	0.079	0.068
	4.5	0.094	0.089	0.082	0.074
30 000	3.5	0.059	0.057	0.050	0.042
	4.0	0.072	0.066	0.061	0.054
	4.5	0.074	0.073	0.068	0.059

Table 13. Model monochromatic magnitude brightening at λ4250 Å as a function of He/H, $T_{\rm eff}$ and $\log g$.

$T_{\rm eff}$	$\log g$	He/H		
		0.2	0.5	1.0
[K]	[dex]	ΔM_{4250} [mag]		
17 000	3.5	–0.013	–0.046	–0.089
	4.0	–0.011	–0.039	–0.075
	4.5	–0.009	–0.031	–0.061
19 000	3.5	–0.017	–0.052	–0.112
	4.0	–0.017	–0.055	–0.100
	4.5	–0.010	–0.047	–0.087
21 000	3.5	–0.015	–0.055	–0.107
	4.0	–0.016	–0.059	–0.113
	4.5	–0.016	–0.058	–0.111
23 000	3.5	–0.013	–0.048	–0.093
	4.0	–0.015	–0.055	–0.106
	4.5	–0.016	–0.058	–0.112
25 000	3.5	–0.007	–0.040	–0.085
	4.0	–0.002	–0.042	–0.090
	4.5	–0.007	–0.050	–0.100
27 000	3.5	–0.010	–0.039	–0.074
	4.0	–0.002	–0.038	–0.077
	4.5	–0.015	–0.051	–0.094
30 000	3.5	–0.010	–0.033	-0.047
	4.0	–0.020	–0.047	–0.084
	4.5	–0.023	–0.047	–0.087

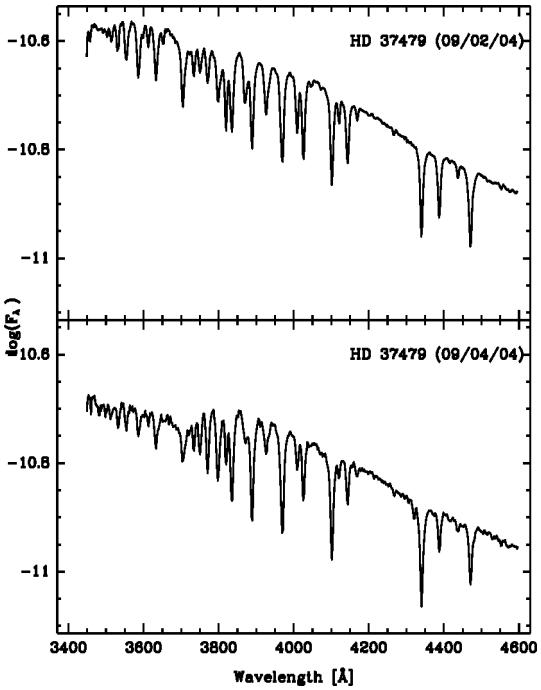

Fig. 6. Line variations observed in the spectrum of HD 37479. The Balmer continuum appears in emission in the spectrum taken in Sep. 2, 2004.

HD 37017 displays a similar behaviour as HD 37479 while HD 64740 does not show appreciable variations for the observing dates.

6. Discussion

The BCD spectrophotometric classification system has shown to be a useful tool to determine fundamental parameters for He-weak stars. To this end, we can use the calibrations of the BCD (λ_1, D) parameters obtained from stars near the Sun.

It is well-known that some He-weak stars display photometric and spectroscopic variations and this fact might influence the determinations of fundamental parameters. However, taking into account that we have observed many of the program stars only once, it is interesting to stress the good agreement found between the fundamental parameters obtained with the BCD system and with other techniques corresponding to data taken in different dates and probably at different phases. Then we may suggest that, in general, the variations due to chemical inhomogenities do not introduce significant changes on the BD of He-weak stars. However, it would be necessary to study in detail those highly variable objects where temperature fluctuations or variations of the magnetic field might be plaussible. Contrary to the He-weak group, He-strong stars show large discrepancies among the $T_{\rm eff}$ values found in the literature. There are several arguments that can account for these discrepancies: a) methods based on the Kurucz' (1979) line blanketed solar composition models can only lead to an approximate flux calibration but, if we do not have a gravity indicator, it is impossible to choose the temperature uniquely (Adelman & Pyper 1985); b) the use of Hβ and Hγ equivalent widths combined with $T_{\rm eff}$ calibrations and/or theoretical Balmer line fittings are uncertain since these lines might be filled by emission or be variable; c) Geneva colours are affected by the He-overabundance and, furthermore, calibration problems may also be present due to the lack of data for hot stars. Zboril et al. (1997) have shown that the [U-B] index of the Geneva photometric system is affected by the enhanced He/H ratio, which affects the b-f and b-b He transitions. Due to these difficulties, the mentioned methods lead to somewhat uncertain $T_{\rm eff}$ determinations.

In this work we have shown that the BCD calibrations lead to overestimated values of $T_{\rm eff}$ for the He-strong stars, since they are actually made for objects with He/H ≈ 0.1. However, if care is made at identifying the genuine continuum flux levels, as indicated in Sect. 5.4, we can still measure the BCD parameter D. This parameter not only well-represents the actual Balmer jump of He-strong stars but also reflects closely the true effective temperature of the star and their H/He ratio when it is used in combination with results of NLTE models. An alternative way to determine the effective temperature of He-strong stars could be the use of the integrated flux method, where the determination of the angular diameter θ is almost insensitive to the type, or quality, of model atmosphere used in the near-IR region. The difference between $T_{\rm eff}$(BCD) and $T_{\rm eff}$(IF) translated into BD difference δD may then produce an estimate of the He/H ratio in these objects.

For the He-strong stars, the Balmer jump might be affected by changes in He/H ratios rather than by changes of the photospheric temperature. When increasing the abundance of He, stellar atmospheres of B stars become less opaque due to the transparency of He I in the visible continuum and the reduction of the relative number of H absorbing atoms. Direct calculations of the κ^+/κ^-, total continuum absorption coefficient ratio at the Balmer discontinuity, show that this effect is slightly stronger for κ^- than for κ^+. This leads to smaller values of D for He-strong stars than for stars with standard He abundance. However, it can still be noted that the He abundance increase may concern only a fraction f of the apparent stellar hemisphere. The fit of observed energy distributions with models should then use both He/H and f as free parameters. The presence of helium patches could be explained in terms of the so-called Oblique Rotator Model. The enhancement of He/H ratio might also give rise to a flux excess in the Balmer continuum originating a second component of the BD in emission.

6.1. Evolutionary status of the studied stars

In order to obtain an insight on the evolutionary status of the He-weak and He-strong stars studied in this work, we plot in Fig. 7 $M_{\rm bol}$ vs. $\log T_{\rm eff}$. For He-strong stars we have taken into account the $T_{\rm eff}$ values derived with NLTE models. The isochrones are for normal stars of metal content typical for the solar vicinity, $Z = 0.02$, and were calculated by Bressan et al. (1993). Some ages t(yr), in logarithm scale, are shown in the figure and the curves are spaced by steps of 0.1 dex.

There is a clear distinction made by the effective temperature, which separates the He-strong from He-weak stars. However, most He-weak and He-strong objects are in the Main Sequence phase.

Since in Fig. 7 there is a well-marked separation between He-weak and He-strong stars according to their effective temperatures, we are tempted to conclude that stars do not evolve from He-weak to He-strong, or viceversa. The separation between these stellar classes seems to be due mainly to mass-effective temperature related phenomena. In fact, the known He-variable star HD 125823, which is located between the two He-peculiar groups, shows alternatively He-w/He-s features. This object could provide important clues to disentangle the evolutionary status of the He-peculiar stars.

Our sample of objects is too small to derive correlations between the star magnetic field and its fundamental

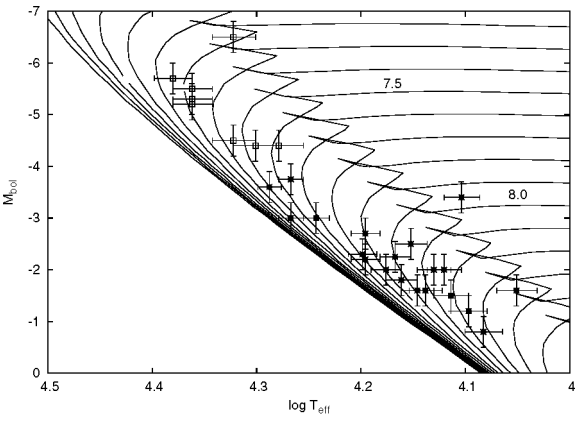

Fig. 7. HR-diagram for He-weak stars (dots) according to BCD fundamental parameters. We also include the He-strong objects (squares) taking into account, in this case, the $T_{\rm eff}$ derived from NLTE models. Isochrones are from Bressan et al. (1993). The ages range from $10^{6.6}$ to 10^{10} yr with steps of $\Delta \log t = 0.1$.

parameters. However our determinations of fundamental parameters and ages are in very good agreement with those estimated by Kochukhov & Bagnulo (2006). These authors find that the surface magnetic flux of CP stars increases with stellar age and mass, and correlates with the rotation period.

7. Conclusions

Several reviews and papers have highlighted the difficulties of obtaining the fundamental parameters of CP stars. Often, the determination of effective temperatures and surface gravities of CP stars by means of photometry and model fittings are more complex than for normal stars.

The main purpose of this work is to estimate the fundamental parameters of 28 helium-peculiar stars using the BCD spectrophotometric system. The advantage of the BCD system is that it provides simultaneously spectral types, $T_{\rm eff}$, $\log g$ and bolometric and absolute magnitudes. All these quantities are obtained from only two parameters drawn from low-resolution spectra which are not affected by ISM and circumstellar absorptions, and the techniques at obtaining them avoid the spectral regions that are strongly perturbed by chemical anomalies of He-peculiar stars. Besides, the effective temperature and surface gravity thus obtained are related to deeper atmospheric layers than those where, on average, the spectral lines are formed, since the BCD quantities are obtained from the visible continuum spectrum.

We confirm that the BCD spectrophotometric system gives reliable effective temperatures, surface gravities and absolute magnitudes for He-weak stars. Not only are $T_{\rm eff}$ values in very good agreement with those obtained with the UBV, multicolour and Geneva photometry, but also with the IRFM and LTE line-blanketed models. Surface gravities show an excellent agreement with values derived from HIPPARCOS parallaxes and stellar evolutionary tracks. The absolute magnitudes also agree with the values obtained from the HIPPARCOS parallaxes and the mean discrepancy between both methods is on average ± 0.3 mag.

Particular attention is payed in this paper to the effective temperature of He-strong stars. The He-strong stars are He-variable and this variability not only affects the intensity of He and H lines, but also the apparent distribution of continuum fluxes. These changes can originate the difficulties of determining the effective temperatures of He-strong stars that were discussed in this work. The determination of the BCD parameter D, which quantifies the Balmer jump, avoids these inconveniences. Nevertheless, the parameter D is a function of the He/H abundance ratio. To specify this dependence, we have calculated non-LTE model atmospheres. We have obtained thus a relation $D = D$(He/H) and could determine the effective temperature of the studied He-strong stars by model fitting. The results show that the higher the He/H ratio, the smaller D. From these models it is also apparent that increased values of He/H are accompanied by brighter fluxes in the Paschen continuum. We have also found that the model fitting produces much lower effective temperatures than expected from the $T_{\rm eff} = T_{\rm eff}(\lambda_1, D)$ BCD calibrations, which actually suit to stars with abundance ratios He/H ≈ 0.1. We have then proposed a method of determining the He/H of He-strong stars, which is based on the mentioned $D = D$(He/H) relation and on two distinct $T_{\rm eff}$ determinations, one coming from the up to now used (λ_1, D) calibration, and the other, which could be the integrated-flux method.

We have observed the He-strong star HD 37479, which underwent a rather strong variation in the visible spectrum in an interval of 2 days. Although the fitting procedure of classical stellar atmosphere models with the observed energy distributions would suggest an apparent variation of the effective temperature, a careful determination of the D parameter shows that this quantity does not vary significantly. We note that in the BCD system D can be constant over a large range of λ_1 parameters, which may reflect the fact that the observed spectrophotometric variations correspond to changes in the structure of possible exophotospheric layers, as in Be stars. In fact, Be stars can sometimes exhibit spectrophotometric changes implying constancy of the total absolute magnitude $M_{\rm V}$ (Moujtahid et al. 1998).

Since the brightening of the Paschen continuum is on average not stronger than some $\Delta M_{4250} \approx -0.10$ mag, the BCD calibration can still be a useful tool to obtain a rough estimate of the absolute magnitudes of He-strong stars.

A first insight on the evolutionary status of He-weak and He-strong stars was obtained. Both types of He-peculiar stars seem to be in the Main Sequence evolutionary phase. The He-strong stars are situated roughly in the $T_{\rm eff} \gtrsim 19\,000$ K region of the HR diagram, while the He-weak are in the $T_{\rm eff} \lesssim 19\,000$ K zone of the HR diagram for B-type stars. More precise $M_{\rm bol}$ determinations for a large number of stars are needed to give a deeper insight on the evolutionary status.

Due to the variability observed in the He-strong group, equivalent widths of hydrogen and helium lines are given. Data for the He-strong star HD 66765 are reported for the first time. Although we have obtained a "normal" He/H ratio for this star, we should consider that this object was reported as a variable He-strong star by Wiegert & Garrison (1998).

Acknowledgements. This work was partially supported by the Agencia de Promoción Científica y Tecnológica (BID 1728 OC/AR PICT 03-12720) and the Programa de Incentivos G11/073 of the National University of La Plata. Y.F. acknowledges financial support from the Belgian Federal Science Policy (projects IAP P5/36 and MO/33/018). This work has made use of CDS data base. We would like to thank our referee Dr. Mathys for his numerous comments and suggestions which considerably helped to improve our manuscript.

References

Adelman, S. J., & Pyper, D. M. 1985, A&AS, 62, 279
Barbier, D., & Chalonge, D. 1941, Ann. Astrophys., 4, 30
Blackwell, D. E., & Shallis, M. J. 1977, MNRAS, 180, 177
Bressan, A., Fagotto, F., Bertelli, G., & Chiosi, C. 1993, A&AS, 100, 647
Bychkov, V. D., Bychkova, L. V., & Madej, J. 2003, A&A, 407, 631
Cayrel de Strobel, G., Hauck, B., Francois, P., et al. 1992, A&AS, 95, 273

Chalonge, D., & Divan, L. 1952, Ann. Astrophys., 15, 201
Chalonge, D., & Divan, L. 1973, A&A, 23, 69
Chalonge, D., & Divan, L. 1977, A&A, 55, 117
Cidale, L. S., Zorec, J., & Tringaniello, L. 2001, A&A, 368, 160
Dimitrijević, M. S., & Sahal-Brechot, S. 1984, JQSRT, 31, 301
Dimitrijević, M. S., & Sahal-Brechot, S. 1990, A&AS, 82, 519
Divan, L. 1979, in Spectral Classification of the Future, ed. Mc Carthy, Philip, Coyne, Vatican Observatory, IAU Coloq., 47, 247
Divan, L., & Zorec, J. 1982, ESA-SP, 177, 101
Flower, P. J. 1977, A&A, 54, 31
Freudenstein, S. A., & Cooper, J. 1978, ApJ, 224, 1079
Gerbaldi, M., Hauck, B., & Morguleff, N. 1974, A&A, 30, 105
Glagolevskij, Y. V. 2002, Bull. Spec. Astrophys. Obs., 53, 33
Golay, M. 1972, Vistas in Astronomy, 14, 13
Gómez, A. E., Luri, X., Grenier, S., et al. 1998, A&A, 336, 953
Hauck, B., & North, P. 1982, A&A, 114, 23
Hauck, B., & North, P. 1993, A&A, 269, 403
Hubeny, I., & Lanz, T. 1995, ApJ, 439, 875
Hubrig, S., North, P., & Mathys, G. 2000, ApJ, 539, 352
Hunger, K., & Groote, D. 1999, A&A, 351, 554
Jaschek, C., & Jaschek, M. 1987a, The Classification of Stars (Cambridge University Press), 173
Jaschek, C., & Jaschek, M. 1987b, A&A, 171, 380
Johnson, H. L., & Mitchell, R. I. 1975, Rev. Mex. Astron. Astrofis., 1, 299
Kaufmann, J. P., & Theil, U. 1980, A&AS, 41, 271
Kochukhov, O., & Bagnulo, S. 2006, A&A, 450, 763
Kroll, R. 1987, A&A, 181, 315
Kurucz, R. 1979, ApJS, 40, 1
Kurucz, R. 1992, CD-ROM Nos. 19–21, Cambridge Mass.: Smithsonian Astrophysisical Observatory
Lanz, T. 1985, A&A, 144, 191
LeBlanc, F., Michaud, G., & Babel, J. 1994, ApJ, 431, 388
Leckrone, D. S., Fowler, J. W., & Adelman, S. J. 1974, A&A, 32, 237
Leone, F., & Manfrè, M. 1997, A&A, 320, 257
Leone, F., Catalano, F. A., & Malaroda, S. 1997, A&A, 325, 1125
Mégessier, C. 1988a, A&A, 206, 74
Mégessier, C. 1988b, A&AS, 72, 551
Moon, T. T., & Dworetsky, M. M. 1985, MNRAS, 217, 305
Moujtahid, A., Zorec, J., Hubert, A. M., et al. 1998, A&AS, 129, 289
Napiwotzki, R., Schönberner, D., & Wenske, V. 1993, A&A, 268, 653
North, P., Jaschek, C., Hauck, B., et al. 1997, Proc. ESA Symp., Hipparcos – Venice 97, Venice, Italy (July 1997), ESA SP-402, 239
Osmer, P. S., & Peterson, D. M. 1974, ApJ, 187, 117
Proffitt, C. R., Brage, T., Leckrone, D., et al. 1999, ApJ, 512, 942
Renson, P., Gerbaldi, M., & Catalano, F. A. 1991, A&AS, 89, 429
Shore, S. N., & Brown, D. N. 1987, A&A, 184, 219
Sokolov, N. A. 1998, A&AS, 130, 215
Sokolov, N. A. 1995, A&AS, 110, 553
Stepień, K., & Dominiczak, R. 1989, A&A, 219, 197
Theodossiou, E., & Danezis, E. 1991, A&AS, 183, 91
Vetö, B., Hempelmann, A., Schöneich, W., & Stahlberg, J. 1991, Astron. Nachr., 312, 133
Walborn, N. 1983, ApJ, 268, 195
Wiegert, P., & Garrison, R. F. 1998, JRASC, 92, 134
Zboril, M., North, P., Glagolevskij, Y. V., & Betrix, F. 1997, A&A, 324, 949
Zboril, M., & North, P. 1999, A&A, 345, 244
Zorec, J., Frémat, Y., & Cidale, L. S. 2005, A&A, 441, 235
Zorec, J. 1986, Ph.D. Thesis, Université de Paris, France
Zorec, J., & Briot, D. 1991, A&A, 245, 150

Online Material

Table 1. Program He-weak (top) and He-strong (botton) stars. In the first two columns we give the star identifiers. Column 3 shows the date of observation. The peculiarity class, and the average quadratic effective magnetic field are presented in Cols. 4 and 5 and were taken from Bychkov et al. (2003).

HD	HR	Date dd/mm/yy	Peculiarity	$\langle B_e \rangle$ Gauss
5737	280	01/09/04	SrTi He-w	324.0
		03/09/04		
		04/09/04		
19400	939	01/09/04	He-w	206.7
22470	1100	01/09/04	Si He-w	732.9
22920	1121	30/09/04	Si4200 He-w	307.1
		01/10/04		
23408	1149	03/09/04	Hg He-w	410.0
28843	1441	03/09/04	Si He-w	344.2
49333	2509	03/09/04	Si He-w	618.4
		01/10/04		
49606	2519	01/10/04	MnHgSi He-w	916.0
51688	2605	01/10/04	Hg He-w	550.2
57219	2790	04/09/04		–
		18/01/06		
74196	3448	18/01/06	He-w	–
125823	5378	18/01/06	Si He-w	469.3
142301	5912	01/10/04	Si He-w	2103.6
142990	5942	02/09/04	He-w	1304.3
		30/09/04		
144334	5988	01/10/04	Si He-w	783.2
144661	5998	01/10/04	He-w	542.0
144844	6003	01/10/04	Si He-w	318.1
162374	6647	01/10/04	He-w	269.8
175362	7129	03/09/04	SiMn He-w	3569.9
202671	8137	01/09/04	SrTi He-wm	183.0
37017	1890	01/09/04	He-s	1488.1
		30/09/04		
37479	1932	02/09/04	He-s	1907.9
		04/09/04		
37776	BD-01 1005	04/09/04	He-s	1259.7
58260	CD-36 3578	18/01/06	He-s	2291.2
60344	CD-23 5673	18/01/06	He-s	334.9
64740	3089	03/09/04	He-s	571.9
		30/09/04		
66765	CD-47 3537	18/01/06	He-s	–
264111	BD+04 1447	18/01/06	He-s	–

Table 2. He-weak stars: measured (λ_1,D) BCD quantities and the corresponding fundamental parameters: $T_{\rm eff}$, $\log g$, spectral type, $M_{\rm V}$, and $M_{\rm bol}$ determined using the calibrations of (λ_1, D) for OB stars of solar He/H ratio.

HD	λ_1 Å	D dex	$T_{\rm eff}$ K	$\log g$ dex	Sp.T	$M_{\rm V}$ mag	$M_{\rm bol}$ mag
5737	32.74	0.281	12700	2.95	B6III	−2.5	−3.4
19400	48.30	0.320	13000	3.90	B6-7V	−0.8	−1.5
22470	58.68	0.296	14000	4.21	B6V	−0.3	−1.6
22920	46.10	0.277	14200	3.80	B6IV	−1.5	−2.5
23408	39.02	0.408	11250	3.20	B9III	−1.1	−1.6
28843	50.67	0.273	14700	3.95	B5IV	−1.1	−2.2
49333	61.20	0.250	15800	4.23	B5V	−0.7	−2.3
49606	46.53	0.340	13500	3.80	B6IV	−1.2	−2.0
51688	49.98	0.340	12500	3.95	B7-8IV	−0.6	−1.2
57219	51.91	0.193	18500	3.92	B2.5IV	−2.0	−3.7
74196	54.78	0.299	13750	4.13	B6V	−0.5	−1.6
125823	57.64	0.184	19400	4.10	B2V	−1.7	−3.6
142301	65.60	0.252	15700	4.30	B5V	−0.7	−2.2
142990	67.21	0.208	18500	4.27	B3V	−1.2	−3.0
144334	63.76	0.280	14500	4.30	B5-6V	−0.4	−1.8
144661	60.31	0.273	15000	4.23	B5V	−0.5	−2.0
144844	65.60	0.346	12100	4.32	B8V	+0.4	−0.8
162374	51.11	0.247	15700	3.95	B5V	−1.3	−2.7
175362	64.75	0.219	17500	4.25	B3V	−1.0	−3.0
202671	44.37	0.303	13200	3.70	B6IV	−1.3	−2.0

Note: The λ_1 parameter is given in $\lambda - 3700$ Å.

Table 3. He-weak stars: our determinations of fundamental parameters: $T_{\rm eff}$, θ, $F_{\rm bol}$, $M_{\rm bol}$ and the $E(B-V)$ color excess used for the ISM extinction correction applying the integrated-flux method.

HD	$T_{\rm eff}$(IF) K	θ(rad) $\times 10^{-10}$	$F_{\rm bol}$ $\times 10^{-7}$	$M_{\rm bol}$ mag	E_{B-V} mag
5737	12490 ± 143	17.6 ± 0.2	10.6 ± 0.6	–3.1 ± 0.4	0.00
57219	18286 ± 125	8.9 ± 0.1	12.5 ± 0.5	–3.8 ± 0.3	0.05
125823	17594 ± 172	12.8 ± 0.2	22.2 ± 1.7	–2.9 ± 0.2	0.01
142301	15084 ± 84	8.8 ± 0.1	5.7 ± 0.2	–1.6 ± 0.4	0.12
144334	15099 ± 77	8.1 ± 0.1	4.8 ± 0.2	–1.6 ± 0.3	0.10
144661	13421 ± 121	7.6 ± 0.5	2.7 ± 0.4	–0.4 ± 0.2	0.09
144844	12448 ± 50	10.1 ± 0.1	3.5 ± 0.1	–0.9 ± 0.2	0.12

Table 4. Comparison of the BCD effective temperatures with those determined by other authors for the program He-weak stars. Column 1 gives the HD number; Col. 2, our $T_{\rm eff}$(BCD) values; Col. 3, $T_{\rm eff}$(G) (Glagolevskij 2002) determined from the parameters Q in the UBV system and X in the multicolour system; Col. 4, $T_{\rm eff}$(KB) determined by Kochukhov & Bagnulo (2006) using the calibration of the Geneva photometry (Golay 1972) and the method suggested by Hauck & North (1993); Col. 5: $T_{\rm eff}$(HG) from Hunger & Groote (1999) using the IRFM, Col. 6: $T_{\rm eff}$(L) obtained by Lanz (1985) using the IRFM, Col. 7: $T_{\rm eff}$(HN) from Hauck & North (1993) using the Geneva photometry, and Col. 8, other values of $T_{\rm eff} \pm \Delta T$ found in the literature, most of them determined by model fitting.

HD	$T_{\rm eff} \times 10^3$ K						
	BCD	G	KB	HG	L	HN	Others
5737	12.7 ± 0.5	13.50 ± 0.3	13.2 ± 0.4	14.4 ± 0.1	–	–	13.6 ± 0.2[a]
							14.0[b]
19400	13.0 ± 0.5	12.90 ± 0.3	–	–	–	–	13.3 ± 0.5[a]
							13.9[c]
22470	14.0 ± 0.5	13.45 ± 0.3	13.0 ± 0.4	13.5 ± 0.4	13.79 ± 0.14	14.25	13.4 ± 0.5[a]
22920	14.2 ± 0.5	14.40 ± 0.3	13.9 ± 0.4	14.3 ± 0.3	–	–	14.1 ± 0.5[a]
23408	11.2 ± 0.5	12.30 ± 0.3	12.0 ± 0.4	–	–	13.80	–
28843	14.7 ± 0.5	14.53 ± 0.3	13.9 ± 0.4	15.0 ± 0.5	14.80 ± 0.19	15.28	–
49333	15.8 ± 0.5	16.60 ± 0.3	16.4 ± 0.5	15.7 ± 0.4	15.94 ± 0.22	16.81	–
49606	13.5 ± 0.5	13.80 ± 0.3	–	–	–	–	14.8[b]
51688	12.5 ± 0.5	13.05 ± 0.3	–	–	–	–	–
57219	18.5 ± 0.5	16.35 ± 0.3	–	–	–	–	17.1[d]
74196	13.7 ± 0.5	13.30 ± 0.3	–	14.2 ± 0.6	–	–	–
125823	19.4 ± 0.5	19.53 ± 0.3	17.7 ± 0.5	18.4 ± 0.4	19.01 ± 0.23	19.60	–
142301	15.7 ± 0.5	16.50 ± 0.3	15.6 ± 0.4	15.9 ± 0.3	15.99 ± 0.15	17.26	–
142990	18.5 ± 0.5	17.80 ± 0.3	16.5 ± 0.5	16.9 ± 0.5	18.02 ± 0.23	–	–
144334	14.5 ± 0.5	15.40 ± 0.3	14.7 ± 0.4	15.2 ± 0.5	14.58 ± 0.23	16.25	–
144661	15.0 ± 0.5	15.00 ± 0.3	–	–	–	–	–
144844	12.1 ± 0.5	12.30 ± 0.3	–	–	–	–	–
162374	15.7 ± 0.5	17.30 ± 0.3	–	16.1 ± 0.3	17.84 ± 0.22	17.37	–
175362	17.5 ± 0.5	17.00 ± 0.3	16.5 ± 0.4	–	16.38 ± 0.20	18.24	16.5[e]
202671	13.2 ± 0.5	14.10 ± 0.3	–	–	–	–	13.1 ± 0.2[a]

[a] Leone & Manfré (1997) or Leone et al. (1997), [b] Cayrel De Strobel et al. (1993), [c] Jaschek & Jaschek (1987b), [d] Kroll (1987), [e] Megéssier (1988b).

Table 5. He-weak stars: comparison of BCD log g values with those obtained by other authors.

HD	log$g$(*BCD*) dex	log$g$(*HG*) dex	log$g$(*Le*) dex
5737	2.95 ± 0.2	$3.48^{+0.15}_{-0.11}$	3.20 ± 0.10
19400	3.90 ± 0.2	–	3.76 ± 0.25
22470	4.21 ± 0.2	$3.97^{+0.09}_{-0.08}$	4.15 ± 0.25
22920	3.80 ± 0.2	$3.82^{+0.13}_{-0.11}$	3.72 ± 0.25
23408	3.20 ± 0.2	–	–
28843	3.95 ± 0.2	$4.33^{+0.08}_{-0.08}$	4.25 ± 0.25
49333	4.23 ± 0.2	$4.18^{+0.12}_{-0.10}$	4.08 ± 0.25
49606	3.80 ± 0.2	–	3.89 ± 0.25
51688	3.95 ± 0.2	–	–
57219	3.92 ± 0.2	–	–
74196	4.13 ± 0.2	$4.14^{+0.30}_{-0.05}$	–
125823	4.10 ± 0.2	$4.16^{+0.08}_{-0.07}$	–
142301	4.30 ± 0.2	$4.29^{+0.13}_{-0.11}$	–
142990	4.27 ± 0.2	$4.20^{+0.10}_{-0.09}$	–
144334	4.30 ± 0.2	$4.29^{+0.10}_{-0.09}$	–
144661	4.23 ± 0.2	–	–
144844	4.32 ± 0.2	–	–
162374	3.95 ± 0.2	$3.95^{+0.18}_{-0.14}$	–
175362	4.25 ± 0.2	–	3.70 ± 0.10
202671	3.70 ± 0.2	–	3.40 ± 0.10

Column 2: this work; Col. 3: Hunger & Groote (1999); Col. 4: Leone & Manfré (1997) or Leone et al. (1997).

Table 6. He-weak stars: comparison of the BCD absolute visual magnitudes with those derived by other authors. The uncertainties of the values are quoted when they are available.

HD	$M_{\rm V}$(BCD)	$M_{\rm V}$(G)	$M_{\rm V}$(KB)	$M_{\rm V}$(Go)
5737	–2.5 ± 0.3	–2.6	–2.31 ± 0.38	–2.0
19400	–0.8 ± 0.3	–1.0	–	–0.7
22470	–0.3 ± 0.3	–0.1	–0.38 ± 0.26	0.0
22920	–1.5 ± 0.3	–	–1.32 ± 0.37	–1.3
23408	–1.1 ± 0.3	–	–1.54 ± 0.25	–1.3
28843	–1.1 ± 0.3	–0.3	0.06 ± 0.24	0.0
49333	–0.7 ± 0.3	–	–0.51 ± 0.32	–0.5
49606	–1.2 ± 0.3	–	–	–1.0
51688	–0.6 ± 0.3	–1.0	–	–0.8
57219	–2.0 ± 0.3	–	–	–
74196	–0.5 ± 0.3	–	–	–0.4
125823	–1.7 ± 0.3	–1.4	–1.18 ± 0.21	–1.4
142301	–0.7 ± 0.3	-0.8	–0.24 ± 0.37	–0.5
142990	–1.2 ± 0.3	–	–0.74 ± 0.27	–
144334	–0.4 ± 0.3	–0.3	–0.29 ± 0.28	–0.5
144661	–0.5 ± 0.3	–	–	–
144844	0.4 ± 0.3	–	–	–
162374	–1.3 ± 0.3	–	–	–1.4
175362	–1.0 ± 0.3	–1.0	–0.4 ± 0.27	–0.5
202671	–1.3 ± 0.3	–1.4	–	–1.1

Column 2: this work; Col. 3: Glagolevskij (2002); Col. 4: Kochukhov & Bagnulo (2006); and Col. 5: Gómez et al. (1998).

Table 7. He-strong stars: measurements and fundamental parameters derived from the BCD spectrophotometric system.

HD	λ_1 Å	D dex	$T_{\rm eff}$ K	log g dex	Sp.T	$M_{\rm V}$ mag	$M_{\rm bol}$ mag
37017	68.72	0.145	21 700	4.22	B1.5V	–2.0	–4.5
37479	87.77	0.107	25 300	4.30	B0.5V	–2.0	–5.3
37776	74.68	0.107	25 400	4.25	B0.5V	–2.2	–5.5
58260	66.05	0.149	21 400	4.20	B2V	–1.9	–4.4
60344	52.97	0.111	24 600	3.80	B1IV	–3.4	–5.7
64740	77.97	0.115	24 500	4.23	B1V	–2.1	–5.2
66765	60.79	0.160	20 200	4.11	B2V	–2.0	–4.4
264111	54.78	0.092	26 700	3.85	B0IV	–3.7	–6.5

Note: the λ_1 parameters are given in λ – 3700 Å.

Table 8. Stellar parameters for the reference He-strong stars obtained with NLTE model atmospheres. We list the HD numbers (Col. 1), the adopted $T_{\rm eff}$, log g, and He/H ratio (Cols. 2–4, respectively), and $V \sin i$ (Col. 5). $V \sin i$ values are taken from Vetö et al. (1983), Walborn (1983), and Zboril et al. (1999).

HD	$T_{\rm eff}$(NLTE) [K]	log g [dex]	He/H	$V \sin i$ km s^{-1}
37017	21 000	4.50	0.5	95
37479	23 000	4.00	0.5	162
37776	23 000	4.00	0.5	95
58260	19 000	4.00	1.0	45
60344	24 000	4.50	1.0	55
64740	23 000	4.00	0.5	160
66765	20 000	4.00	0.1	100
264111	21 000	4.50	1.0	140

Table 9. Comparison of the BCD effective temperatures with those determined by other authors for the program He-strong stars.

HD	$T_{\rm eff} \times 10^3$ K			
	BCD	G	Z	K
37017	21.7 ± 1.5	20.10 ± 0.3	19.2	21.0
37479	25.3 ± 1.5	22.45 ± 0.3	22.2	23.5
37776	25.4 ± 1.5	23.35 ± 0.3	21.8	26.0
58260	21.4 ± 1.5	19.70 ± 0.3	19.0	–
60344	24.6 ± 1.5	21.90 ± 0.3	21.7	25.0 ± 1.0
64740	24.5 ± 1.5	23.85 ± 0.3	22.7	23.5
66765	20.2 ± 1.5	–	–	–
264111	26.7 ± 1.5	21.60 ± 0.3	23.2	20.0

Column 2: BCD system; Col. 3: Glagolevskij (2002); Col. 4: Zboril et al. (1997); Col. 5: Kaufmann & Theil (1980).

Table 10. Comparison of surface gravity estimates for the He-strong stars.

HD	log$g$(BCD)	log$g$(Z)	log$g$(HG)	log$g$(LCM)	log$g$(K)
37017	4.22 ± 0.2	4.45 ± 0.10	$4.12^{+0.34}_{-0.23}$	4.02 ± 0.25	4.4
37479	4.30 ± 0.2	4.53 ± 0.17	–	3.86 ± 0.25	4.1
37776	4.25 ± 0.2	4.52 ± 0.07	$4.16^{+0.30}_{-0.30}$	4.11 ± 0.25	4.0
58260	4.20 ± 0.2	4.02 ± 0.18	$3.55^{+0.47}_{-0.27}$	3.52 ± 0.25	–
60344	3.80 ± 0.2	4.48 ± 0.18	–	3.50 ± 0.25	3.62
64740	4.23 ± 0.2	4.50 ± 0.06	$4.10^{+0.09}_{-0.08}$	3.80 ± 0.25	3.9
66765	4.11 ± 0.2	–	–	–	–
264111	3.85 ± 0.2	4.54 ± 0.06	–	–	4.0

Column 2: this work; Col. 3: Zboril et al. (1997); Col. 4: Hunger & Groote (1999); Col. 5: Leone et al. (1997); Col. 6: Kaufmann & Theil (1980).

Table 11. Absolute visual magnitudes for the program He-strong stars.

HD	$M_{\rm V}$(BCD)	$M_{\rm V}$(G)	$M_{\rm V}$(KB)	$M_{\rm V}$(Go)
37017	–2.0 ± 0.3	–1.6	–	–2.2
37479	–2.0 ± 0.3	–	–	–
37776	–2.2 ± 0.3	–2.7	–	–2.2
58260	–1.9 ± 0.3	–4.2	–	–3.3
60344	–3.4 ± 0.3	–3.6	–	–2.7
64740	–2.1 ± 0.3	–3.3	-2.15 ± 0.25	–2.5
66765	–2.0 ± 0.3	–	–	–
264111	–3.7 ± 0.3	–	–	–3.1

Columns 2: this work; Col. 3: Glagolevskij (2002); Col. 4: Kochukhov & Bagnulo (2006); and Col. 5: Gómez et al. (1998).

Appendix A: Line equivalent widths of the He-strong stars

Having in mind the strong variations observed in HD 37479 and HD 37017, we considered useful to report line equivalent width measurements for all the program He-strong stars.

We measured equivalent widths (EW) of hydrogen and helium lines in the spectra of the 8 observed He-strong stars and of the variable He-w/He-s star HD 125823 (see Table A.1). We have compared our equivalent width measurements with those found in the literature. From this comparison it comes out that the EWs derived by Walborn (1983) are, in most cases, larger than ours by factors ranging from 1.3 to 2, except for the He I lines observed in HD 37479 (Sep. 4, 2004) and HD 264111. The discrepancies between Zboril's et al. (1997) EWs and ours are about 10 to 15%. The largest difference is found for HD 37479 (Sep. 2, 2004), our EWs are larger by a factor of 1.4.

Table A.1. Equivalent widths in Å of hydrogen and helium lines for the program He-strong stars and the Helocentric Julian Date.

HD	HJD	Hγ	He I			
	–2453000		λ4026	λ4144	λ4387	λ4471
37017	249.9020	5.48	2.05	1.28	1.37	2.19
37017	278.7787	7.26	1.17	0.74	0.76	1.43
37479	250.8538	3.20	3.08	2.10	2.12	3.32
37479	252.8841	4.16	2.13	1.30	1.35	2.32
37776	252.8756	4.00	2.29	1.52	1.42	2.53
58260	754.7432	4.28	2.12	1.34	1.30	2.33
60344	755.7009	4.16	1.95	1.44	1.35	2.42
64740	251.9172	4.20	1.97	1.14	1.13	2.08
64740	278.8559	4.50	1.63	1.33	1.29	2.18
66765	755.7666	5.78	1.39	0.78	0.91	1.81
125823	754.8733	6.25	0.46	0.23	0.22	0.51
264111	755.6925	4.29	2.13	1.63	1.51	2.45